Int. J. Heat Mass Transfer. Vol. 34, No. 11, pp. 2703–2713, 1991
Printed in Great Britain

0017–9310/91 $3.00 + 0.00

Characteristics of lithium chloride in rotary heat and mass exchangers

J. J. RAU, S. A. KLEIN and J. W. MITCHELL
Solar Energy Laboratory, University of Wisconsin–Madison, Madison, WI 53706, U.S.A.

(*Received* 24 *April* 1990 *and in final form* 27 *November* 1990)

Abstract—The behavior of the air–water vapor–desiccant system is of central interest for modeling rotary heat and mass exchangers in desiccant cooling systems. Lithium chloride is commonly used as desiccant in commercial systems, primarily because of the low humidities that can be obtained. This paper provides relationships to describe the sorption equilibria of the air–water vapor–LiCl system. Rotary heat and mass exchangers are described by two conservation laws and two transfer equations. They form a system of two coupled non-linear hyperbolic partial differential equations and two ordinary differential equations. Since the isotherms and isopiestics of LiCl exhibit discontinuities, conventional numerical methods that solve this system cannot be used. A modified method based on the finite difference model by Maclaine-cross (A theory of combined heat and mass transfer in regenerators, Ph.D. Thesis, Monash University (1979)) is presented. This method predicts the outlet conditions of the air streams and determines temperature and moisture content profiles of the matrix. A description of the complex physical behavior of rotary dehumidifiers using LiCl is presented.

INTRODUCTION

THIS PAPER investigates the thermodynamic characteristics of lithium chloride (LiCl) as a sorptive agent for water vapor. In a system of LiCl and water vapor, both physical absorption and chemisorption (forming of hydrates) are involved. Lithium chloride can sorb water vapor as a solid (anhydrous salt or monohydrate crystals) or as a liquid after the sorbed water has dissolved the solid into an aqueous solution, called a deliquescent desiccant.

Lithium chloride is a hygroscopic salt with high moisture capacity, easy regenerability and high chemical stability. It is the most widely used desiccant in commercial rotary dehumidifiers because of its outstanding ability to achieve very low humidities even at high moisture content. The high moisture capacity of LiCl (relative to micro-porous adsorbents such as silica gel or molecular sieves) is an asset which is limited only if the LiCl liquifies and drips off the supporter when the dilution becomes too high.

In commercial rotary dehumidifiers, LiCl salt is impregnated on a supporter which provides an extended surface through which the LiCl crystals may be finely dispersed. The supporter also helps hold the LiCl solution up to a certain degree of dilution. The LiCl impregnated supporter is referred to as the 'matrix', while the air carrying the water vapor is referred to as the 'fluid'. In rotary dehumidifiers, the sorbent matrix is mounted in a frame in the form of a wheel that rotates in a housing. The air streams are separated by seals and flow counter to each other in the axial direction.

MODEL FORMULATION

Figure 1 shows a schematic diagram of a rotary heat and mass exchanger (RHMX). The sorbent material, i.e. the LiCl impregnated on its supporter, is arranged in a rotating cylindrical wheel of depth L. The two counterflow air streams that pass through the wheel are physically separated and flow in the axial direction through parallel passages. The cool and moist process stream corresponds to period $j = 1$ while the hot regenerating stream corresponds to period $j = 2$. The coordinate system is defined as shown in Fig. 1. For each period, the axial coordinate z is defined to be positive in the flow direction. Therefore, its direction is reversed at the beginning of each period. The circumferential coordinate Θ can be regarded either as an angular position or time since the rotation speed is constant. Θ is set to zero at the beginning of each period. The RHMX may be asymmetric, i.e. the duration of the two periods Θ_j may differ; their sum gives the time of one complete rotation. The RHMX may be unbalanced with different air flow rates for the process and regeneration streams.

The mathematical model for the performance is based on a set of standard assumptions [1, 2].

(1) Energy and water transport between matrix and fluid can be described by overall (or lumped) transfer coefficients. There is no transfer flux coupling through thermal diffusion or Dufor effects.

(2) The transfer coefficients remain constant throughout the exchanger; the matrix geometry is uniform.

NOMENCLATURE

A_j exchange area of the matrix in period j [m^2]
c_f specific heat of wet fluid [J K^{-1} (kg dry air)$^{-1}$]
c_m specific heat of the wet matrix [J K^{-1} (kg dry sorbent)$^{-1}$]
F_1, F_2 characteristic potential for equilibrium between fluid and matrix
h_s heat of sorption [J (kg water)$^{-1}$]
$h_{t,j}$ overall heat transfer coefficient for period j [W m^{-2} K^{-1}]
$h_{w,j}$ overall mass transfer coefficient for period j [(kg water) m^{-2} s^{-1}]
h_{wv} enthalpy of water vapor [J (kg water)$^{-1}$]
I enthalpy of the matrix [J (kg dry sorbent)$^{-1}$]
i enthalpy of the air [J (kg dry air)$^{-1}$]
Le_j Lewis number of period j, $h_{t,j}/c_f h_{w,j}$
$\dot{m}_j$ dry air mass flow rate of period j [(kg dry air) s^{-1}]
$NTU_{w,j}$ number of transfer units for mass transfer
t_f, t_m temperature of fluid and matrix [°C]
W water content of matrix [kg (kg dry sorbent)$^{-1}$]
W_{mono} water content of pure monohydrate [kg (kg dry sorbent)$^{-1}$]
w humidity ratio of air [(kg water) (kg dry air)$^{-1}$]
w_m humidity ratio of fluid in equilibrium with matrix [kg (kg dry air)$^{-1}$]
Δw_m difference in equilibrium humidity ratio on either side of a discontinuity
x dimensionless distance, z/L
z coordinate in axial direction [m].

Greek symbols
Γ_j ratio of dry matrix mass flow rate to fluid flow rate
ζ dimensionless time, $NTU_{w,j}\tau/\Gamma_j$
Θ time or circumferential coordinate [s]
Θ_j duration of period j [s]
ξ dimensionless axial position, $NTU_{w,j}x$
τ dimensionless time, Θ/Θ_j.

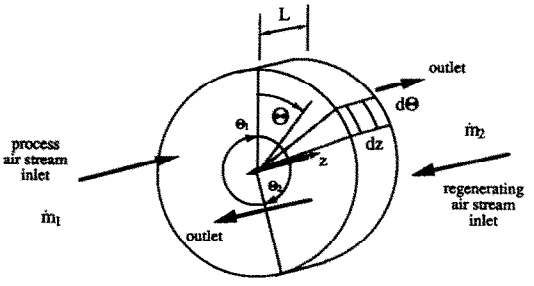

FIG. 1. Schematic diagram of the RHMX showing the coordinate system.

(3) Heat conduction and water diffusion in the matrix and fluid are negligible in the angular and axial directions.

(4) Heat and mass capacity in the fluid is negligible compared to the capacity in the matrix.

(5) The inlet streams are well mixed; their temperature and humidity are constant and uniform when they enter the RHMX.

(6) The RHMX operates adiabatically overall. Fluid and matrix properties do not vary with the radius of the wheel.

(7) The pressure drop along the flow length is negligible; the fluid flows with constant velocity.

(8) There is no mixing or carry over between the two fluid streams.

The first assumption allows the use of a simple transfer rate equation with a linear driving force between the matrix and fluid bulk properties. The lumped transfer coefficients are usually found by experiment. Convective transfer coefficients can only be used if the solid phase resistance can be neglected.

By defining dimensionless coordinates and the NTU of heat and mass exchangers

$$x = \frac{z}{L}, \quad \tau = \frac{\Theta}{\Theta_j} \tag{1a,b}$$

$$NTU_{w,j} = \frac{h_{w,j}A_j}{\dot{m}_j} \tag{2}$$

and by combining all the parameters into one dimensionless group

$$\Gamma_j = \frac{M_d}{\dot{m}_j\Theta_j} \tag{3}$$

the governing equations for the RHMX for each period may be written as

$$\Gamma_j\frac{\partial W}{\partial \tau} + \frac{\partial w}{\partial x} = 0 \tag{4a}$$

$$\Gamma_j\frac{\partial I}{\partial \tau} + \frac{\partial i}{\partial x} = 0 \tag{4b}$$

$$\frac{\partial w}{\partial x} = NTU_{w,j}(w_m - w) \tag{5a}$$

$$\frac{\partial i}{\partial x} = NTU_{w,j}[Le_j\, c_f(t_m - t_f) + h_{wv}(w_m - w)]. \tag{5b}$$

These equations represent a coupled set of two hyperbolic wave equations and two first-order equations for seven unknown fluid and matrix properties as

functions of distance and time. These properties are the water content, enthalpy and temperature of fluid and matrix and the air humidity in equilibrium with the matrix. Additional thermodynamic relationships are needed to specify the properties. These are the equilibrium air humidity as a function of matrix temperature and water content

$$w_m = f(W, t_m) \tag{6}$$

the enthalpy of the matrix as a function of temperature and water content

$$I = f(W, t_m) \tag{7}$$

and the enthalpy of the fluid

$$i = f(w, t_f). \tag{8}$$

Most of these relationships are nonlinear, as evident in the property data from refs. [1–4]. In addition, the equilibrium relationship is discontinuous. Within the temperature range of 19.1–93.5°C, there can exist: (i) solid crystals of anhydrous LiCl and monohydrate; (ii) a saturated solution containing monohydrate; or (iii) dilute solution as seen in the phase diagram for the LiCl–water system shown in Fig. 2. Above 93.5°C, monohydrate crystals are unstable and the saturated solution contains anhydrous salt. Figure 3 shows the step-like shape of the isotherms and its dependence on temperature.

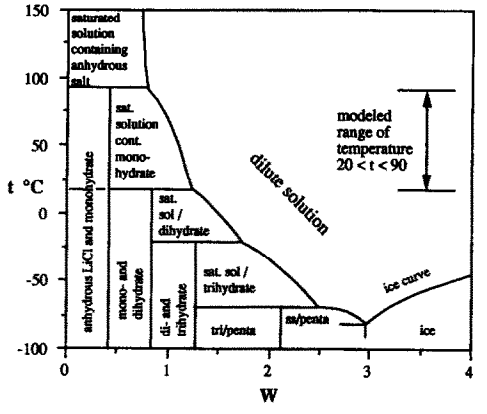

FIG. 2. Phase diagram of the LiCl–water system.

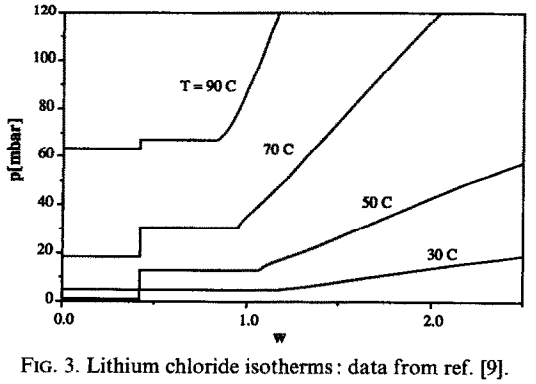

FIG. 3. Lithium chloride isotherms: data from ref. [9].

The boundary conditions for the system are

$$w(x = 0) = w_{j,in} \tag{9a}$$

$$i(x = 0) = i_{j,in}. \tag{9b}$$

The initial conditions for the matrix properties are periodic and therefore unknown. The reversal condition at the boundary where the matrix leaves the regenerating period 2 and enters the process period 1 is

$$W(\tau_1 = 0) = W(\tau_2 = 1) \tag{10a}$$

$$I(\tau_1 = 0) = I(\tau_2 = 1) \tag{10b}$$

and at the transition from period 1 to period 2

$$W(\tau_2 = 0) = W(\tau_1 = 1) \tag{11a}$$

$$I(\tau_2 = 0) = I(\tau_1 = 1) \tag{11b}$$

where subscript τ indicates the current period.

The conservation laws (4) and transfer equations (5) together with the thermodynamic relationships (6)–(8) and the boundary and periodic initial conditions (9)–(11) form a complete set of algebraic and differential equations that determines the behavior of the RHMX. This model can also be applied to fixed beds that are periodically processed and regenerated.

A numerical model which solves the governing differential equations of the rotary heat and mass exchanger was developed by Maclaine-cross [5] for sorbents with continuous isotherms. In this work, this model was modified to accommodate desiccants with discontinuous isotherms. This resulting model described in this paper does not rely on the validity of the analogy between heat and mass transfer nor does it require the assumption of equilibrium between the matrix and the fluid as originally modeled by Maclaine-cross and Banks [3]. The heat/mass transfer analogy assumption, which is appropriate for some sorbents, is invalid for desiccants such as LiCl which have discontinuities in the isotherm.

In developing the mathematical solution, new non-dimensional variables for position and time are introduced

$$\xi = NTU_{w,j}x \tag{12a}$$

$$\zeta = NTU_{w,j}\tau/\Gamma_j. \tag{12b}$$

Substituting these dimensionless variables into the governing heat and mass conservation (4) and mechanism (5) equations and using the chain rule to replace enthalpies with temperatures as the dependent variables results in the following set of equations:

$$\frac{\partial W}{\partial \zeta} + \frac{\partial w}{\partial \xi} = 0 \tag{13a}$$

$$\frac{\partial I}{\partial t_m}\frac{\partial t_m}{\partial \zeta} + \frac{\partial I}{\partial W}\frac{\partial W}{\partial \zeta} + c_f\frac{\partial t_f}{\partial \xi} + h_{wv}\frac{\partial w_f}{\partial \xi} = 0 \tag{13b}$$

$$\frac{\partial w}{\partial \xi} = w_m - w \tag{13c}$$

$$\frac{\partial t_f}{\partial \xi} = Le(t_m - t_f). \tag{13d}$$

Transforming the dependent variables from enthalpies to temperatures simplifies the analysis. However, this transformation causes a major limitation of this model. Cast in terms of temperatures, rather than enthalpies, it is no longer possible to account for the latent heat due to the phase change from anhydrous LiCl and water to monohydrate at 93.5°C. This latent heat is independent of any sorption or desorption process. Hence the matrix enthalpy changes discontinuously with temperature and the derivative $(\partial I/\partial t_m)_W$ becomes infinite. For this reason, the following model can only simulate the performance of the RHMX with hydrates of LiCl in the temperature range of 19.1–93.5°C. If LiCl remains in dilute solution, the model is applicable for all temperatures.

In the numerical solution to equations (13), the matrix is discretized in time and space using a staggered mesh shown in Fig. 4. The matrix and fluid dependent variables are evaluated at different nodes in the mesh. Each grid element is regarded as a cross flow exchanger. The equations are applied for the center of the grid element (represented with a tilde (~)) to produce second-order accuracy for the solution scheme. The resulting finite difference equations can be written in matrix form as

$$\begin{bmatrix} \frac{1}{\Delta\xi} & 0 & 0 & 0 \\ 0 & \frac{1}{\Delta\xi} & 0 & \frac{1}{\Delta\zeta} \\ 0 & \frac{1}{\Delta\xi} & 0 & 0 \\ \frac{c_f}{\Delta\xi} & \frac{h_{wv}}{\Delta\xi} & \frac{\partial I}{\partial t_m}\frac{1}{\Delta\zeta} & \frac{\partial I}{\partial W}\frac{1}{\Delta\zeta} \end{bmatrix} \times \begin{bmatrix} t_{f\,i+1,\tilde{k}} - t_{f\,i,\tilde{k}} \\ w_{i+1,\tilde{k}} - w_{i,\tilde{k}} \\ t_{m\,\tilde{i},k+1} - t_{m\,\tilde{i},k} \\ W_{\tilde{i},k+1} - W_{\tilde{i},k} \end{bmatrix} = \begin{bmatrix} Le[t_m - t_f]_{\tilde{i},\tilde{k}} \\ 0 \\ [w_m - w_f]_{\tilde{i},\tilde{k}} \\ 0 \end{bmatrix}. \tag{14}$$

The differences $[t_m - t_f]_{\tilde{i},\tilde{k}}$ and $[w_m - w_f]_{\tilde{i},\tilde{k}}$ must be known at the center of the element. To keep the second-order accuracy, the arithmetic mean is used to provide an estimate

$$[t_m - t_f]_{\tilde{i},\tilde{k}} = \tfrac{1}{2}(t_{m\,\tilde{i},k+1} + t_{m\,\tilde{i},k}) - \tfrac{1}{2}(t_{f\,i+1,\tilde{k}} + t_{f\,i,\tilde{k}}) \tag{15a}$$

$$[w_m - w_f]_{\tilde{i},\tilde{k}} = \tfrac{1}{2}(w_{m\,\tilde{i},k+1} + w_{m\,\tilde{i},k}) - \tfrac{1}{2}(w_{f\,i+1,\tilde{k}} + w_{f\,i,\tilde{k}}). \tag{15b}$$

These equations are implicit. The term, $w_{m\,\tilde{i},k+1}$, is eliminated by using a Taylor expansion for $W_{\tilde{i},k+1}$

$$W_{\tilde{i},k+1} = W_{\tilde{i},k} + \left[\frac{\partial W}{\partial t_m}\right]_{w_m}(t_{m\,\tilde{i},k+1} - t_{m\,\tilde{i},k}) + \left[\frac{\partial W}{\partial w_m}\right]_{t_m}(w_{m\,\tilde{i},k+1} - w_{m\,\tilde{i},k}). \tag{16}$$

Eliminating $w_{m\,\tilde{i},k+1}$, the resulting explicit matrix equation can be written

$$\begin{bmatrix} t_{f\,i+1,\tilde{k}} - t_{f\,i,\tilde{k}} \\ w_{i+1,\tilde{k}} - w_{i,\tilde{k}} \\ t_{m\,\tilde{i},k+1} - t_{m\,\tilde{i},k} \\ W_{\tilde{i},k+1} - W_{\tilde{i},k} \end{bmatrix} = \begin{bmatrix} \frac{1}{\Delta\xi} + \frac{Le}{2} & 0 & -\frac{Le}{2} & 0 \\ 0 & \frac{1}{\Delta\xi} & 0 & \frac{1}{\Delta\zeta} \\ 0 & \frac{1}{\Delta\xi} + \frac{1}{2} & -\frac{1}{2}\left[\frac{\partial w_m}{\partial t_m}\right]_W & -\frac{1}{2}\left[\frac{\partial w_m}{\partial W}\right]_{t_m} \\ \frac{c_f}{\Delta\xi} & \frac{h_{wv}}{\Delta\xi} & \frac{\partial I}{\partial t_m}\frac{1}{\Delta\zeta} & \frac{\partial I}{\partial W}\frac{1}{\Delta\zeta} \end{bmatrix}^{-1} \times \begin{bmatrix} Le[t_{m\,\tilde{i},k} - t_{f\,\tilde{i},k}] \\ 0 \\ w_{m\,\tilde{i},k} - w_{f\,\tilde{i},k} \\ 0 \end{bmatrix}. \tag{17}$$

This Taylor expansion for $W_{\tilde{i},k+1}$, however, is not feasible at a discontinuity where a phase change occurs since the derivatives $\partial w_m/\partial t_m$ and $\partial w/\partial w_m$ become infinite.

As the humidity changes pass through the bed, there are discontinuities in the isotherm which result in 'jumps' in equilibrium matrix water content with distance. To account for the discontinuities, $w_{m\,\tilde{i},\tilde{k}}$ is evaluated as the mean of $w_{m\,\tilde{i},k}$ and $w_{m\,\tilde{i},k+1}$ where $w_{m\,\tilde{i},k+1}$ is known to be after the jump and can be approximated by $w_{m\,\tilde{i},k+1} = w_{m\,\tilde{i},\tilde{k}} \pm \Delta w_m(t_m)$. The sign depends on the period (process +, regenerating period −). The change in w_m from position k to $k+1$ due to changes in temperature is neglected

$$[w_m - w_f]_{\tilde{i},\tilde{k}} = w_{m\,i,k} \pm \tfrac{1}{2}\Delta w_m - w_{f\,i,k}\tfrac{1}{2}(w_{f\,i+1,k} - w_{f\,i,k}). \tag{18}$$

The resulting system of equations is much simpler than the original equations for the continuous system

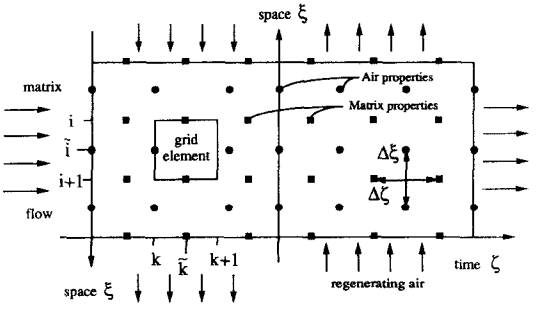

FIG. 4. Staggered mesh used in the analysis.

$$\begin{bmatrix} t_{f\,i+1,k}-t_{f\,i,k} \\ w_{i+1,k}-w_{i,k} \\ t_{m\,\tilde{i},k+1}-t_{m\,\tilde{i},k} \\ W_{\tilde{i},k+1}-W_{\tilde{i},k} \end{bmatrix} =$$

$$\begin{bmatrix} \frac{1}{\Delta\xi}+\frac{Le}{2} & 0 & -\frac{Le}{2} & 0 \\ 0 & \frac{1}{\Delta\xi} & 0 & \frac{1}{\Delta\zeta} \\ 0 & \frac{1}{\Delta\xi}+\frac{1}{2} & 0 & 0 \\ \frac{c_f}{\Delta\xi} & \frac{h_{wv}}{\Delta\xi} & \frac{\partial I}{\partial t_m}\frac{1}{\Delta\zeta} & \frac{\partial I}{\partial W}\frac{1}{\Delta\zeta} \end{bmatrix}^{-1}$$

$$\times \begin{bmatrix} Le[t_{m\,\tilde{i},k}-t_{f\,\tilde{i},k}] \\ 0 \\ w_{m\,\tilde{i},k}-w_{f\,\tilde{i},k}\pm\frac{1}{2}\Delta w_m \\ 0 \end{bmatrix}. \quad (19)$$

The boundaries of the humidity interval for the jump at W_{mono} are the equilibrium humidity of the system of anhydrous LiCl and monohydrate w_{am} and the equilibrium humidity of the saturated solution w_{ms}. The boundaries of the humidity interval of the jump at zero water content are zero and w_{am}. If the humidity of the air lies within one of these intervals and the matrix has reached the corresponding water content (zero or W_{mono}), water vapor can neither be sorbed nor desorbed. An increment in sorbed water will cause the equilibrium humidity to jump so that it is higher than the air humidity and thereby reverses the driving force. If an arbitrarily small amount of water is desorbed, the equilibrium humidity will correspondingly jump below the air humidity and reverse the driving force again. Sorption or desorption processes come to a halt. Thus there is heat exchange only. In this case, the humidity of the fluid and the water content of the matrix do not change and the mass conservation and transfer rate equations are satisfied identically and drop out of the system of equations (19). The simplified set of equations for heat exchange only is

$$\begin{bmatrix} \frac{1}{\Delta\xi}+\frac{Le}{2} & -\frac{Le}{2} \\ \frac{c_f}{\Delta\xi} & \frac{\partial I}{\partial t_m}\frac{1}{\Delta\zeta} \end{bmatrix} \begin{bmatrix} t_{f\,i+1,k}-t_{f\,i,k} \\ t_{m\,\tilde{i},k+1}-t_{m\,\tilde{i},k} \end{bmatrix}$$

$$= \begin{bmatrix} Le(t_{m\,\tilde{i},k}-t_{f\,i,k}) \\ 0 \end{bmatrix} \quad (20)$$

The algorithm thus has to distinguish four cases:

Case I. The matrix water content is not near a discontinuity. The conventional numerical equations (17) are used. To calculate the outlet temperatures and moisture contents appearing on the left-hand side of equation (17) with second-order accuracy, all of the state property functions on the right-hand side must be evaluated as functions of t_m, W, t_f and w at the center of the grid element $(\tilde{i}, \tilde{k})$. Since these values are not known, the values for the inlet temperature and moisture content are used first. Then the outlet temperatures and moisture contents are computed and the mean of the inlet and outlet values is used as a second approximation to evaluate the state property functions.

Case II. The sorption (or desorption) process reaches the discontinuity. The air humidity is higher than the upper equilibrium humidity of the discontinuity (or below the lower equilibrium humidity) so the dehumidification process (regeneration) can proceed and cross the discontinuity. To find out when the algorithm has reached the grid element where the jump occurs, the outlet temperatures and moisture contents are evaluated as in Case I and then checked to determine if the matrix water content has changed into the new state. In that case the algorithm switches over to the new set of finite difference equations (19) and the temperatures and moisture contents are re-evaluated.

Case III. The sorption (or desorption) process reaches the discontinuity and stagnates there since the fluid humidity is within the humidity interval of the jump. The water content of the matrix is set equal to either W_{mono} or zero. The element mass balance is used to determine the 'outlet' fluid humidity. Temperatures are determined using the results of the conventional equations (17). This introduces a small error which is acceptable since this case can at most occur once for every space loop.

Case IV. The matrix water content is at the discontinuity. The air humidity lies within the jump interval. There is heat exchange only and equations (20) are employed.

The algorithm that was developed moves through the grid with an inner space loop and an outer time loop. Within the space loop, the grid element 'outlet' states are computed according to the above four cases. The algorithm was implemented within the MOSHMX program, developed by Maclaine-cross [5], which contains algorithms to provide an estimate of the solution at zero grid size by quadratically extrapolating the results from three progressively smaller grid sizes. Two values for the time increments are used corresponding to the two wave fronts that propagate through the matrix with different speeds. Initially a small time increment is selected in order to follow the fast front. After the front passes, as detected by the norm of the matrix temperature change of all grid elements, a larger time step is then used. The entire algorithm is iterated so that the matrix state at the beginning of the process period is the same as that at the end of the regenerating period. Overall mass and enthalpy balances for the air streams are taken as the convergence criteria. At the end of the period the matrix state vectors for water content and temperature are reversed since the axial coordinate is defined positive in the air flow direction.

SINGLE BLOW SIMULATION RESULTS

The finite difference method of this paper was used to calculate the change in temperature and water content with flow length and time for a specified initial state of the matrix. The dehumidifier was simulated in a single blow mode from an initial regenerated state to complete exhaustion in order to gain an understanding of the physical behavior of the dehumidifier. The parameters chosen for this calculation were $NTU = 5$ and $Le = 1$.

The inlet conditions of the fluid were chosen to be $t_{f,in} = 25°C$ and $w_{in} = 0.015$. The matrix may initially consist of either a dilute solution of LiCl, a saturated solution or solid LiCl, i.e. a mixture of anhydrate and monohydrate. For this calculation, the initial water content of the matrix was taken to be $W = 0.3$. Therefore, the matrix initially contains both monohydrate and anhydrate. The initial matrix temperature was chosen to be $t_m = 75°C$. The matrix and fluid temperatures and humidity profiles are shown in Figs. 5 and 6.

In the beginning of the dehumidification process, the high matrix temperature is very quickly cooled down to 58°C. The relative time is given in terms of the number of time steps with the numerical time step of $\Delta\zeta = 0.5$. This change in temperature results from a fast wave that propagates through the matrix. The matrix temperature remains at 58°C where a phase change from monohydrate to saturated solution occurs.

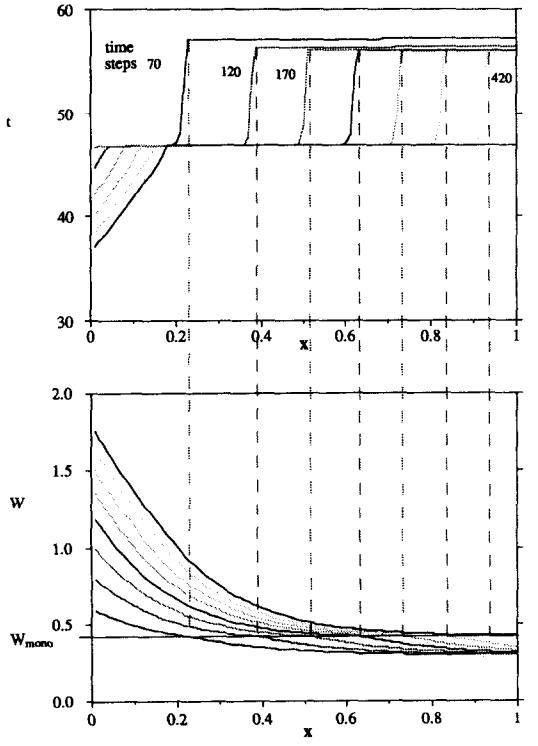

FIG. 5. Matrix water content and temperature profile wave front corresponding to change from solid to saturated solution.

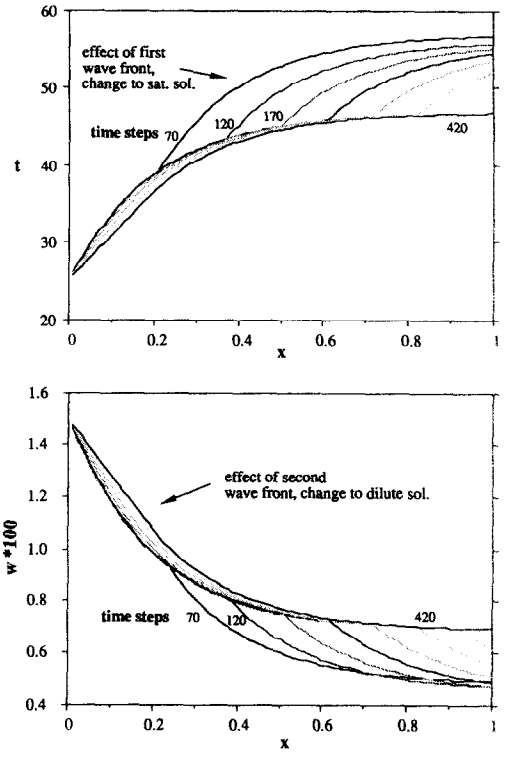

FIG. 6. Fluid properties during change from solid to saturated solution.

During the next time steps (to 420), the LiCl changes from the solid state to saturated solution and crosses the discontinuity at W_{mono}. As expected, the moisture content profiles are not differentiable at W_{mono}; the slopes exhibit a sudden change. On the left-hand side of the jump, the matrix has already changed its state and now contains a saturated solution. Hence the rate of the dehumidification process is slowed due to the suddenly smaller driving force. Less water is sorbed and the heat of sorption is also smaller.

When the matrix undergoes the phase change, the temperature suddenly drops again, now to 47°C, where the latent heat of the mass transfer equals the heat transfer for the sorption process in the saturated solution. The locus of points where this phase change occurs represents another wave front that propagates through the matrix. This wave front is followed by another for which the LiCl becomes a dilute solution and the temperature drops again. The effect of these wave fronts on the fluid properties is shown in Fig. 6.

The resulting air outlet conditions are shown in Fig. 7. There is first a fast wave. Then temperature and humidity remain constant for a short time until the temperature drops as the first wave front moves through the matrix. This behavior results in a low outlet humidity which lasts until the smaller driving force of the saturated solution reverses this effect and

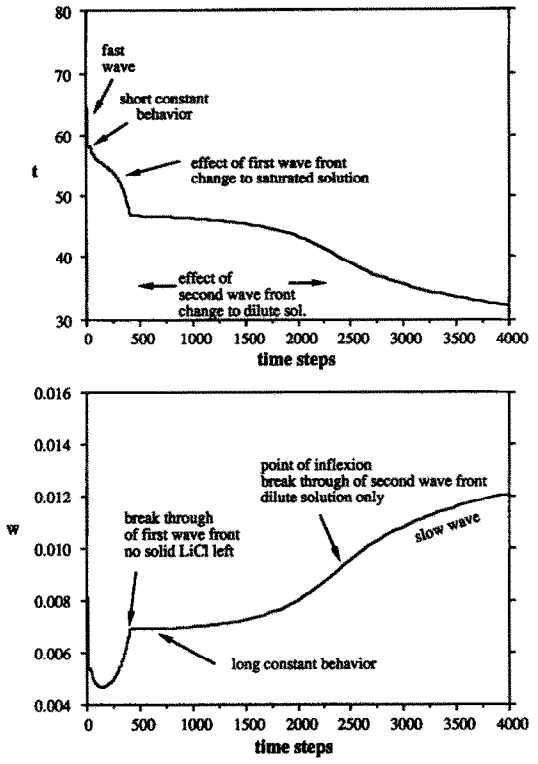

FIG. 7. Air outlet states, wave fronts.

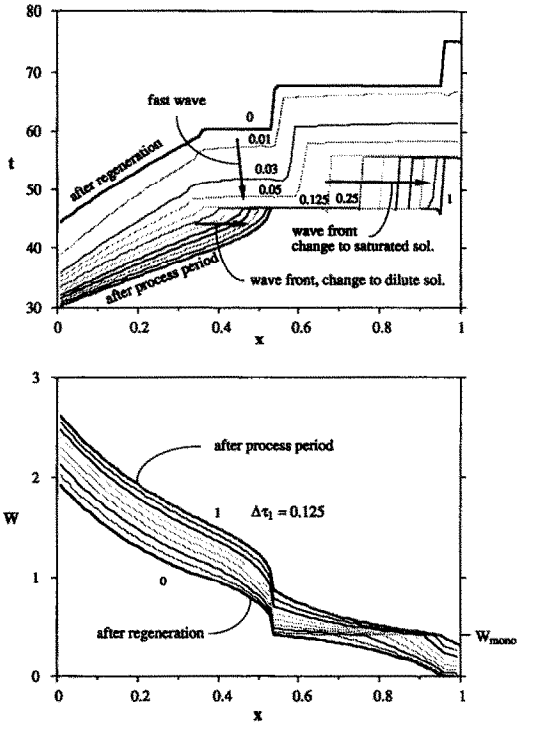

FIG. 8. Steady state of regenerator profiles during process period for $\Gamma_1 = \Gamma_2 = 0.02$.

the humidity increases. After this wave front passes, the humidity and temperature remain constant for a relatively long time. Finally the temperature drops and the humidity increases as the second wave front approaches the end of the dehumidifier.

STEADY-STATE SIMULATION RESULTS

Figure 8 shows the profiles of the matrix properties during the process period as a function of axial position with circumferential position τ as a parameter. For this simulation, the process air inlet conditions were taken to be $t_{f,in} = 25°C$ and $w_{in} = 0.015$ while the regenerating air was taken to be at $t_{f,in} = 75°C$ with a humidity of $w_{in} = 0.008$. As a result, the regenerating air is dry and hot enough to obtain anhydrous LiCl.

The bold lines in Fig. 8 with the highest temperature and with the lowest water content represent the properties of the matrix leaving the regeneration period and entering the process period. The two corresponding bold lines with the lowest temperature and the highest water content identify the state of the matrix leaving the process period and entering the regeneration period. At all other circumferential positions, the matrix states will be between these limiting lines.

In the process period, the temperature profiles quickly shift to lower temperatures due to the fast wave during the first few time steps (thin lines). The water content changes only slightly (no corresponding thin lines). The completely anhydrous matrix near the end of the dehumidifier ($x = 0.95$–1) immediately starts to sorb water. Hence, the wave front in the temperature profile that separates the water-free matrix with heat exchange only from the mixture of anhydrate and monohydrate moves immediately out of the matrix.

After the fast wave has passed ($\tau > 0.1$), the temperature profile shifts to the right without changing its shape significantly. The wave front that represents the phase change to saturated solution almost reaches the end of the dehumidifier before it is reflected back during the regeneration period.

In the regeneration period, the fast wave first increases the temperature, before the wave fronts move slowly back to the left. In this simulation, Γ was taken to be 0.02 which is near the optimum value where the best dehumidification at the outlet state is obtained. For larger values of Γ (lower mass flow rate or faster rotating wheel), the water content profiles after processing and regenerating will be closer together than in Figs. 8 and 9, while the temperature profiles will be roughly the same. The transition from dilute to saturated solution and from saturated solution to solid will be much steeper. The entire regenerator will be similar to three single regenerators in series, one containing dilute solution, one saturated solution and one solid LiCl. The process outlet humidity will be higher because the fast wave takes relatively more time out of the entire period and the initial high temperatures are less favorable to the dehumidification process.

For smaller values of Γ (slower rotating wheel or increased air flow rate), the wave fronts will move faster and may move out of the regenerator before they are reflected back during the regenerating period. If the wave front where the matrix changes to saturated solution moves out of the regenerator before the end of the period, the dehumidification process near the end of the regenerator, where the final outlet humidity is obtained, will be slowed down or will even stop. The profiles in Fig. 8 represent an operation near the optimum because this wave front comes close but does not move out of the dehumidifier.

PROCESS DIAGRAMS FOR LiCl

A method of characteristics has often been employed to represent the processes in desiccant dehumidifiers. It is possible to combine the temperature and humidity variables into two characteristic potentials, termed F_1 and F_2, which decouple the governing equations [1, 3, 5]. These potentials then describe the equilibrium processes that would occur in a dehumidifier with no heat or mass transfer resistances. Representation of these characteristic lines on psychometric coordinates provides insight into the behavior of the desiccant. The lines represent the sorption processes for dehumidifiers with finite heat and mass transfer coefficients. The characteristic potentials are not directly useful in analysis of advanced systems such as staged regeneration but they are useful in indicating the limits of performance of dehumidifiers.

F_1, F_2-Charts for LiCl in dilute LiCl solution have been developed by Maclaine-cross [5]. Lines of constant F_j are obtained by integrating the following expression:

$$\left[\frac{\partial w}{\partial t}\right]_{F_j} = \frac{c_m \dfrac{\partial W}{\partial t} - \dfrac{1}{2}\dfrac{\partial W}{\partial t}\dfrac{\partial i}{\partial t}}{2h_s \dfrac{\partial W}{\partial w}} + (-1)^j \times \left\{\left\{\frac{c_m \dfrac{\partial W}{\partial t} - \dfrac{1}{2}\dfrac{\partial W}{\partial t}\dfrac{\partial i}{\partial t}}{2h_s \dfrac{\partial W}{\partial w}}\right\}^2 - \frac{\dfrac{\partial W}{\partial t}\dfrac{\partial i}{\partial t}}{h_s \dfrac{\partial W}{\partial w}}\right\}^{1/2}. \tag{21}$$

Integration of equation (21) leads to some difficulties for LiCl in either the saturated solution or solid state because the partial derivatives of the matrix properties may become zero or infinite. The critical term in this equation is $\partial W/\partial w$. Three cases have to be distinguished: the first case corresponds to finite $\partial W/\partial w$, the second one corresponds to infinite $\partial W/\partial w$ and in the last case $\partial W/\partial w$ equals zero.

Case I. All derivatives are finite as it is in the case for the dilute solution. Lines of constant F_j can be obtained by numerically integrating equation (21) with a fourth-order Runge–Kutta method.

Case II. The matrix derivatives are infinite. Therefore, $1/(\partial W/\partial w)$ is equal to zero and equation (21) can then be written as

$$\left[\frac{\partial w}{\partial t}\right]_{F_j} = \frac{1}{2}\left[\frac{\partial w}{\partial t}\right]_w - \frac{1}{2h_s}\frac{\partial i}{\partial t} + (-1)^j \sqrt{\left(\left\{\frac{1}{2}\left[\frac{\partial w}{\partial t}\right]_w - \frac{1}{2h_s}\frac{\partial i}{\partial t}\right\}^2 - \frac{1}{h_s}\frac{\partial i}{\partial t}\left[\frac{\partial w}{\partial t}\right]_w\right)} = \frac{1}{2}\left[\frac{\partial w}{\partial t}\right]_w - \frac{1}{2h_s}\frac{\partial i}{\partial t} + (-1)^j \left[\frac{1}{2}\left[\frac{\partial w}{\partial t}\right]_w + \frac{1}{2h_s}\frac{\partial i}{\partial t}\right]. \tag{22}$$

For $j = 1$, $[\partial w/\partial t]_{F_1} = -(1/h_s)(\partial i/\partial t)$ which is finite and negative for w, t values on the discontinuity lines. However, with an arbitrary small step, these lines can be crossed and Case II is no longer valid, i.e. $\partial W/\partial w$ is no longer infinite. Hence there is no impact of the discontinuities on the shape of the lines of constant F_1-potential.

For $j = 2$, $[\partial w/\partial t]_{F_2} = [\partial w/\partial t]_w$. The discontinuity lines, i.e. the isostere for the saturated solution and the isostere for a system of anhydrous LiCl and monohydrate, are also lines of constant F_2.

Case III. At a phase change, the derivative $\partial W/\partial w$ is equal to zero and the terms containing the inverse of this derivative become infinite. Therefore, the other terms in the equation can be neglected and equation (21) can be reduced to

$$\left[\frac{\partial w}{\partial t}\right]_{F_j} = 0 \quad \text{for } j = 1 \tag{23a}$$

$$\left[\frac{\partial w}{\partial t}\right]_{F_j} \to \infty \quad \text{for } j = 2. \tag{23b}$$

This simplification results in horizontal lines for F_1 and vertical lines for F_2 on the psychrometric chart.

Figure 9 shows the F-charts of LiCl over a large temperature and humidity range. The astonishing

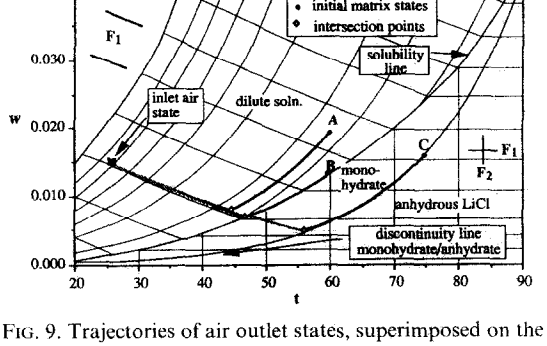

FIG. 9. Trajectories of air outlet states, superimposed on the LiCl F-chart.

result is that the discontinuities cannot be seen in these charts. However, the fact that the lines of constant F-potential do not exhibit any discontinuity does not mean that the F-values do not change significantly. The step changes of the $W(w, t)$ function as seen in Fig. 3 cannot be seen in the lines of constant W. Thus the w, t-discontinuity lines for W may also be discontinuity lines for F_2.

The physical significance of the F-charts can be evaluated by plotting trajectories of the air outlet conditions for single blow simulations. Possible initial matrix states are either a dilute solution of LiCl, a saturated solution, or solid LiCl consisting of anhydrate and monohydrate. These initial states correspond to points in the F-chart that are in the region of dilute solution, on the solubility line or on the discontinuity line that separates the regions for anhydrate and monohydrate as indicated on Fig. 9.

The outlet air in the very beginning will be in equilibrium with these initial points. Hence, all trajectories start out at these initial points. At the end of the process, when the matrix is completely exhausted, the outlet air will be the same as the inlet air. Therefore, the trajectories all end at the point of the inlet air state.

For the first case where the matrix initially contains a dilute solution (point A in Fig. 9), the air outlet states move very fast down along the F_2-line. This corresponds to the initial fast wave that propagates through the matrix. Then the slow wave will shift the outlet states up the F_1-line until they reach the inlet state when the matrix is exhausted. Hence, the intersection point represents the optimum dehumidification that can be obtained under these initial matrix and air inlet conditions. The same behavior is exhibited by desiccants that do not have discontinuous isotherms.

Similar behavior occurs for the matrix initially containing a saturated solution of LiCl, which starts at a point on the solubility line (point B in Fig. 9). The outlet states will stagnate at the intersection point until the wave front that corresponds to the change to dilute solution approaches the end of the dehumidifier and effects the outlet states. Finally the slow wave will move the outlet state up the F_1-line.

In the most complicated case where the matrix is at the equilibrium point of monohydrate and anhydrous LiCl (point C), the matrix will change from solid LiCl to the saturated solution and then to the dilute solution. In this case the air outlet states will also stay constant after the fast wave passed through, but only for a very short time. Then the medium speed wave front that corresponds to the change to saturated solution will first lower the humidity and then increase it as shown in Fig. 7. As a result, the lowest humidity air exits the dehumidifier while this wave front is still propagating through the matrix and not when it breaks through. This point of the trajectory is highly transitory compared to the air conditions after this wave front breaks through. At this point, the air outlet conditions will stay constant for a long time. They are close to the solubility line. Finally, with the next wave front, the air outlet states move up along the F_1-line.

The problem in applying the analogy method for this last case is that the point with the lowest humidity cannot be identified from the F-chart alone. It lies on the F_2-line through the initial matrix state, but it cannot be shown mathematically that it has the same F_1-value. From this analysis it cannot be determined that this is the intersection point. If the matrix at the beginning of the process period contains pure monohydrate or saturated solution, the regenerating air will be in the region of monohydrate. In this case, the intersection point is the intersection of the solubility line and the F_1-line through the process air inlet state.

For both inlet states being in the region of dilute solution, the analogy method can be applied as for continuous sorbents. If the F_2-line of the regenerating air inlet state hits the solubility limit before intersecting with the F_1-line of the process air inlet state, the solubility line will continue the F_2-line and the intersection point of the solubility line and the F_1-line may also be used.

CONCLUSIONS

A model has been developed that simulates a regenerative heat and mass exchanger (RHMX) using LiCl as the desiccant. The results are based on the numerical solution to governing heat and mass transfer relations. Experimental sorption characteristics for the LiCl–water system have been incorporated into the model. The numerical analysis used in the model accommodates discontinuities in the adsorption isotherm. Experiments on sorption in LiCl beds are needed to support the calculated performance results.

To make use of the ability of LiCl to process very dry air, the regeneration period must reactivate the matrix such that anhydrous LiCl is obtained. Then, the reactivation temperature must be high enough such that the temperature dependent equilibrium humidity of solid LiCl is higher than the regenerating air humidity. Temperatures above 93.5°C are practical since anhydrous LiCl can be obtained directly from the saturated solution. Such high regenerating temperatures allow higher regenerating air humidities.

The physical behavior of the RHMX may be described by an initial fast wave and slower subsequent wave fronts that represent the phase changes and propagate through the matrix. These wave fronts have only a small effect on the water content profiles, but due to the large changes of the latent heat, they have a large effect on the temperature profiles. For the change from solid LiCl to saturated solution the water content profiles will exhibit a knee since the driving force for the mass transfer jumps discontinuously.

The fast wave shifts the temperature profiles up or down at the beginning of each period. Then the wave

fronts move the temperature profiles back and forth during the two periods, while the water content profiles are shifted up and down. How far these wave fronts will move depends on the parameter Γ_j. For optimum dehumidification, the wave front where the matrix changes to saturated solution will come close to breaking through. The corresponding value for Γ_j was found to be approximately 0.02.

Psychrometric charts with lines of constant F-potential for LiCl in the solid state, in saturated solution, and in dilute solution were presented. It was shown that the discontinuity lines for the equilibrium water content are also F_2-lines. Trajectories of the outlet states of single blow simulations were used to identify possible intersection points. However, for the case where the matrix initially contains solid LiCl and will change across the discontinuity to saturated solution, the empirical point of lowest humidity of the trajectory cannot be found by intersecting the F-potential lines. As a result, the analogy method can only be applied for sorption processes on the saturated and dilute solution.

REFERENCES

1. J. J. Jurinak, Open cycle desiccant cooling—component models and system simulation, Ph.D. Thesis, University of Wisconsin, Madison (1982).
2. E. Van den Bulck, Design theory for rotary heat and mass exchangers—I. Wave analysis of rotary heat mass exchanger with infinite transfer coefficients, and II. Effectiveness–number of transfer units method for rotary heat and mass exchangers, *Int. J. Heat Mass Transfer* **28,** 1575–1595 (1985).
3. I. L. Maclaine-cross and P. J. Banks, Coupled heat and mass transfer in regenerators—prediction using an analogy with heat transfer, *Int. J. Heat Mass Transfer* **15,** 1225 (1971).
4. C. Chi, Dynamics of fixed bed absorbers, Ph.D. Thesis, I.I.T., Chicago (1968).
5. I. L. Maclaine-cross, A theory of combined heat and mass transfer in regenerators, Ph.D. Thesis, Monash University, Clayton, Victoria, Australia (1979).
6. M. P. Appleby, Crawford, Gordon, Vapour pressure of saturated solutions. Lithium chloride and lithium sulphate, *J. Chem. Soc.* **11,** 1665 (1934).
7. Ch. Slonin und G. F. Hüttig, Die Spezifischen Wärmen, Bildungswärmen der Lithiumhalogendihydrate, *Z. Phys. Chem.* **141,** 55 (1929).
8. N. A. Gokcen, Vapor pressure of water above saturated lithium chloride solution, *J. Am. Chem. Soc.* **73,** 3789 (1951).
9. E. F. Johnson, Molstad, Thermodynamic properties of lithium chloride solutions, *J. Phys. Chem.* **55,** 257 (1951).
10. E. Lange und F. Dürr, Lösungs- und Verdünnungswärmen von Salzen, *Z. Phys. Chem.* **121,** 379 (1926).

CARACTERISTIQUES DU CHLORURE DE LITHIUM DANS LES ECHANGEURS TOURNANTS DE CHALEUR ET DE MASSE

Résumé—Le comportement du système air–vapeur d'eau–dessiccateur est d'un grand intérêt pour la modélisation des échangeurs tournants de chaleur et de masse. Le chlorure de lithium est généralement utilisé comme dessiccateur dans les systèmes commercialisées à cause des faibles humidités que l'on peut obtenir. On donne des formules pour décrire l'équilibre de sorbtion du système air–vapeur d'eau–LiCl. Les échangeurs tournants de chaleur et de masse sont décrits par deux lois de conservation et deux équations de transfert. Elles forment un système de deux équations aux dérivées partielles hyperboliques non linéaires et deux équations différentielles. Puisque les isothermes et les isopiestiques du LiCl montrent des discontinuités, les méthodes numériques conventionnelles ne peuvent être utilisées. On présente une méthode basée sur le modèle de différences finies par Maclaine-cross (A theory of combined heat and mass transfer in regenerators, Ph.D. Thesis, Monash University (1979)). Cette méthode prédit les conditions de sortie de l'air et détermine les profils de température et d'humidité de la matrice. On présente une description du comportement physique complexe des dessiccateurs tournants utilisant LiCl.

EINSATZ VON LITHIUM-CHLORID IN ROTIERENDEN APPARATEN FÜR DEN WÄRME- UND STOFFAUSTAUSCH

Zusammenfassung—Das Verhalten des Entfeuchtungsmaterials ist bei der Modellierung rotierender Apparate für den Wärme- und Stoffaustausch in Kühlsystemen zur Entfeuchtung von zentraler Bedeutung. In kommerziellen Systemen wird als Entfeuchtungsmaterial üblicherweise Lithium-Chlorid eingesetzt, vorwiegend wegen der erzielbaren niedrigen Feuchtigkeiten. Die vorliegende Arbeit liefert Beziehungen zur Beschreibung des Sorptionsgleichgewichts des Systems Luft/Wasserdampf/Lithium-Chlorid. Rotierende Apparate für den Wärme- und Stoffaustausch werden auf der Grundlage von zwei Erhaltungsgleichungen und zwei Übertragungsgleichungen beschrieben. Diese bilden ein System mit zwei gekoppelten nichtlinearen hyperbolischen partiellen Differentialgleichungen und zwei gewöhnlichen Differentialgleichungen. Da die Linien gleicher Temperatur und gleichen Druckes in LiCl Unregelmäßigkeiten zeigen, können herkömmliche numerische Modelle nicht zur Lösung dieses Problems verwendet werden. Es wird ein modifiziertes Verfahren, das auf dem Finite-Differenzen-Modell von Maclaine-cross (A theory of combined heat and mass transfer in regenerators, Ph.D. Thesis, Monash University (1979)) basiert, vorgestellt. Mit dieser Methode können die Austrittsbedingungen der Luftströme vorausberechnet sowie Temperatur- und Feuchtigkeitsprofile der Matrix bestimmt werden. Das komplexe physikalische Verhalten rotierender Entfeuchter mit LiCl wird beschrieben.

ХАРАКТЕРИСТИКИ ХЛОРИДА ЛИТИЯ В РОТАЦИОННЫХ ТЕПЛО- И МАССООБМЕННИКАХ

Аннотация—При моделировании ротациоиных тепло- и массообменников в осушающих охлаждающих системах особый интерес представляют характеристики системы воздух–водяной пар–осушитель. В качестве осушителя в промышленных системах обычно используется хлорид лития прежде всего благодаря возможности получения низкой влажности. В настоящем исследовании приводятся соотношения, описывающие сорбционное равновесие системы воздух–водяной пар–LiCl. Ротационные тепло- и массообменники описываются двумя законами сохранения и двумя уравнениями переноса, которые образуют систему из двух взаимосвязанных нелинейных гиперболических уравнений в частных производных и двух обыкновенных дифференциальных уравнений. Поскольку в изотермах и линиях с одинаковым давлением насыщенного пара LiCl обнаруживаются разрывы, общепринятые методы непригодны для решения данной системы. Предложен модифицированный метод на основе конечно-разностной модели (A theory of combined heat and mass transfer in regenerators, Ph.D. Thesis, Monash University (1979)). Указанный метод позволяет определять условия для потока воздуха на выходе, а также профили температур и влагосодержаний матрицы. Дается описание сложного физического поведения ротационных осушителей, использующих LiCl.